International Journal of Thermophysics, Vol. 28, No. 1, February 2007 (© 2007)
DOI: 10.1007/s10765-007-0158-2

PVT Measurements for Pure Ethanol in the Near-Critical and Supercritical Regions

A. R. Bazaev,[1] I. M. Abdulagatov,[1–3] E. A. Bazaev,[1] and A. Abdurashidova[1]

Received October 18, 2006

The PVT properties of pure ethanol were measured in the near-critical and supercritical regions. Measurements were made using a constant-volume piezometer immersed in a precision thermostat. The uncertainty of the density measurements was estimated to be 0.15%. The uncertainties of the temperature and pressure measurements were, respectively, 15 mK and 0.05%. Measurements were made along various near-critical isotherms between 373 and 673 K and at densities from 91.81 to 497.67 $kg \cdot m^{-3}$. The pressure range was from 0.226 to 40.292 MPa. Using two-phase PVT results, the values of the saturated-liquid and -vapor densities and the vapor pressure for temperatures between 373.15 and 513.15 K were obtained by means of an analytical extrapolation technique. The measured PVT data and saturated properties for pure ethanol were compared with values calculated from a fundamental equation of state and correlations, and with experimental data reported by other authors. The values of the critical parameters (T_C,P_C,ρ_C) were derived from the measured values of saturated densities and vapor pressure near the critical point. The derived values of the saturated densities near the critical point for ethanol were interpreted in term of the "complete scaling" theory.

KEY WORDS: coexistence curve; critical point; equation of state; ethanol; saturated density; vapor pressure.

1. INTRODUCTION

Although ethanol is a common substance and often used for technological and scientific applications, its thermodynamic properties have not been

[1] Institute for Geothermal Problems of the Dagestan Scientific Center of the Russian Academy of Sciences, Shamilya Str. 39, 367003 Makhachkala, Dagestan, Russia.
[2] Present address: Physical and Chemical Properties Division, National Institute of Standards and Technology, 325 Broadway, Boulder, Colorado 80305, U.S.A.
[3] To whom correspondence should be addressed. E-mail: ilmutdin@boulder.nist.gov

very well studied, especially at near-critical and supercritical conditions. Ethanol is a very interesting compound as a constituent of binary mixtures because of its high polarity (highly associated fluid, gas-phase dipole moment at normal boiling point (NBP) is 1.6909 D), and high acentric factor ($\omega = 0.644$). Therefore, the thermodynamic properties of mixtures where ethanol is one of the components are governed by hydrogen bonding which, in contrast to physical interactions, is short-ranged and highly directional. Mixtures of ethanol with other fluids form highly nonideal systems, for example, excess molar properties and critical lines for ethanol solute mixtures exhibit unusually large deviations from ideal mixture behavior. Ethanol is also used as a polar co-solvent in supercritical fluid technologies to enhance the solubility of a solute and to improve the selectivity of the supercritical solvent (effective polar modifiers) [1–8]. Ethanol can be used as a renewable bio-fuel. Therefore, the design of technological equipment utilizing ethanol requires an accurate knowledge of its thermodynamic properties. Due to its high polarity and strong self-association, ethanol has a complex structure and is a challenge to study both experimentally and theoretically. We do not have a sufficient understanding of microscopic properties of associated fluids including the nature of hydrogen bonds and their effect on thermodynamic properties. A deeper understanding of the structure and nature of hydrogen bonding fluids and their effect on the thermodynamic behavior will lead to marked improvements in important practical applications in the environmental, mechanical, chemical, biological, and geothermal industries.

A survey of the literature reveals that measurements of the thermodynamic properties of pure ethanol in the near-critical and supercritical regions are very scarce. Moreover, the available experimental data in the critical region show large discrepancies. Available information on the critical properties of ethanol and saturated densities near the critical point is somewhat sparse and is variable in quality. For example, the differences between critical parameters (T_C, P_C, ρ_C) reported by different authors are as much as 14.3 K, 5.93 MPa, and 57.7 $kg \cdot m^{-3}$, respectively. The differences between the reported values of saturated-liquid and -vapor densities in the critical region are as large as 20–50%.

1.1. *PVT* Measurements in the Critical and Supercritical Regions

Most reported experimental data for the density of pure ethanol cover the temperature range below 373 K. *PVT* properties of pure ethanol above 373 K and at high pressures were reported by several authors [9–15]. Sauermann et al. [13] reported *PVT* properties of ethanol (99.8 vol% purity) in the temperature range from 263 to 483 K and at pressures up to 57 MPa.

Measurements were made with a vibrating tube technique. The maximum uncertainty in density measurements is 0.06%. Lo and Stiel [12] used a constant-volume method to measure the density of ethanol (99.95 mol%) in the temperature range from 473 to 623 K and at pressures up to 69 MPa. The uncertainty of the measurements is 0.4%. The measurements by Tamann and Rühenbeck [14] cover a temperature range from 293 to 673 K and a pressure range from 0.04 to 96 MPa. Kalafati et al. [11] employed a constant volume piezometer to measure the density of ethanol (96 vol% purity) in the temperature range from 423 to 573 K and at pressures up to 20 MPa. The uncertainty in the specific volume measurements is within 0.1–0.3%. Golubev et al. [9] and Zolin et al. [10] reported the densities of liquid ethanol (99.89%, 0.07% H_2O and 0.04% organic compounds) in the temperature range from 194 to 571 K and at pressures up to 50 MPa. Measurements were performed with a hydrostatic weighing method. The uncertainty in density measurements is about 0.1% at high densities (above 300 $kg \cdot m^{-3}$) and 0.3% at lower densities. Using an extrapolation technique, the values of saturated liquid densities were determined in the temperature range from 194.7 to 506.4 K. Popov and Malov [15] measured the densities of ethanol in the temperature range from 273 to 473 K and at pressures up to 30 MPa by using two cylindrical piezometers (with volumes of 10.903 and 11.019 cm^3) inserted in a high precision thermostat. The uncertainty in density measurements is about 0.5%.

1.2. Vapor Pressures and Saturated-Liquid and -Vapor Densities

Vapor-pressure data for pure ethanol at high temperatures (above 373 K) were reported by various authors [10,11,13,16–31]. Saturated-liquid and -vapor densities for ethanol (above 373 K) were also reported [10,11,13,21,27,32–40]. Very limited data are available for the saturated vapor of ethanol. Only six data sources were found for saturated vapor densities [10,21,27,37–39] in the critical region. Vapor pressures and saturated-liquid and -vapor densities for ethanol in the critical region were reported by Mousa [27], but the measurements are unreliable. Other thermodynamic properties such as the isochoric heat capacity [37,39–42], sound speed [43], and enthalpy [31,44,45] of pure ethanol in the critical and supercritical regions were also reported.

1.3. Equation of State and Correlations

A fundamental equation of state for the Helmholtz energy $A(V, T)$ of pure ethanol is reported by Dillon and Penoncello [46]. This equation of state represents the thermodynamic properties of pure ethanol in the

temperature range from 250 to 650 K at pressures up to 280 MPa and densities to 893.73 $kg \cdot m^{-3}$. The uncertainty of the calculated values of density is 0.2%, and that of the saturated pressure and saturated density is 0.5%. Ambrose and Walton [22] developed an equation for the vapor pressures of pure ethanol. Cibulka [47] reported a correlation equation for saturated-liquid densities of pure ethanol. This correlation reproduced experimental values of the saturated-liquid densities in the temperature range from the normal melting point (159 K) to 508.2 K with a standard deviation of 0.161%. A Storbridge-type equation of state for ethanol was also developed by Sauermann et al. [13]. They also reported a Wagner-type vapor-pressure equation for ethanol. A low-temperature (below 490 K) correlation for the saturated-liquid density was developed by Hales and Ellender [32].

1.4. Critical Parameters

Polikhronidi et al. [37] and Gude and Teja [48] have reviewed the critical properties (T_C,P_C,ρ_C) of pure ethanol. A large scatter of the available critical parameter values of ethanol is found in the literature. An analysis of the reported values of the critical parameters for pure ethanol reveals that all of the reported data for the critical temperature lie between 506.9 and 521.2 K, the critical density between 228.3 and 286 $kg \cdot m^{-3}$, and the critical pressure between 6.1309 and 12.06 MPa. Recently Polikhronidi et al. [37] reported values of the critical temperature and critical density for ethanol from calorimetric (C_V) measurements in the critical region. The results are $\rho_C = 282.33 \pm 2\ kg \cdot m^{-3}$ and $T_C = 514.44 \pm 0.02$ K. These critical parameters are close to the values ($\rho_C = 275 \pm 2\ kg \cdot m^{-3}$, $T_C = 514.0 \pm 0.2$ K, and $P_C = 6.137 \pm 0.02$ MPa) recommended by Gude and Teja [48]. The recommended values of Dillon and Penoncello [46] are $\rho_C = 276\ kg \cdot m^{-3}$, $T_C = 513.9$ K, and $P_C = 6.148$ MPa. A majority of the published values for the critical temperature for ethanol lie between 513.9 and 516.7 K, the critical density lies within 275–277 $kg \cdot m^{-3}$, and the critical pressure between 6.13 and 6.40 MPa. This is one of the reasons why reported saturated-liquid and -vapor densities show large discrepancies (up to 50% and more for the saturated vapor and up to 10–20% for saturated-liquid densities) in the critical region.

Thus, the main objective of this paper is to provide accurate *PVT* data in the critical and supercritical regions, the phase boundary (P_S,T_S,ρ_S), and critical properties (T_C,P_C,ρ_C) data for ethanol. The present measurements focused on the temperature range from 373 to 673 K, at pressures up to 40 MPa and densities from 91.81 to 497.67 $kg \cdot m^{-3}$. The present results expand considerably the existing *PVT* database at near-critical and

supercritical conditions for pure ethanol. We also provided a comprehensive analysis of all available experimental PVT data sets, and saturated and critical property data for pure ethanol by detailed comparisons to determine the reliability of published data and correlations. This work is a part of a continuing program on volumetric (PVT) and caloric ($C_V VT$) property measurements of alcohols and their aqueous solutions in the critical and supercritical regions. The present PVT apparatus has been previously used for accurate measurements on other pure fluids and aqueous solutions in the critical and supercritical regions (Abdulagatov et al. [49–53], Bazaev et al. [54–58], and Rabezkii et al. [59]).

2. EXPERIMENTAL PROCEDURE

The apparatus used for PVT measurements of ethanol is similar to that used in previous papers [49–59] to measure PVT properties of pure methanol, *n*-alkanes, and their aqueous solutions in the critical and supercritical regions. Detailed descriptions of the apparatus and the experimental procedure, and uncertainty assessment have been described in our previous publications [49–59]. The measurements were made using the constant-volume method, with an extraction of the sample from the piezometer under isothermal conditions. The inner volume of the piezometer was calculated by taking into consideration corrections of the elastic pressure deformation and thermal expansion. The internal volume of the piezometer was previously calibrated by filling it with pure water. The volume of the piezometer $V_{T_0 P_0} = m(H_2O)/\rho(H_2O)$ at temperature $T_0 = 673.15\,K$ and pressure $P_0 = 38.35\,MPa$ was calculated from the well established (IAPWS-95 formulation, Wagner and Pruß [60]) density $\rho(H_2O)$ and mass of the water $m(H_2O)$. The derived value of the volume at these conditions was $V_{T_0 P_0} = (32.56 \pm 0.02)\,cm^3$. It is necessary to know the volume of the piezometer, V_{PT} at a given temperature T and pressure P, for the purpose of calculating densities $\rho(T, P) = m/V_{PT}$. Variations of the piezometer volume V_{PT} with temperature T and pressure P were calculated by using the thermal expansion coefficient of the piezometer material, $\alpha = 1.56 \times 10^{-5}\,K^{-1}$, and the pressure expansion coefficient of the piezometer, $\beta = 3.51 \times 10^{-5}\,MPa^{-1}$. All masses were determined with an uncertainty of $5 \times 10^{-4}\,g$. The volume of the piezometer at a given temperature T and pressure P was measured with an uncertainty of 0.01–0.02%.

The fluid under study was thermostated in a double-wall air bath. The fluid temperature (ITS-90) was measured with a $10\,\Omega$ platinum resistance thermometer (PRT-10). The maximum uncertainty in the measured temperature was 15 mK. The temperature inside the thermostat was maintained uniform within 5 mK with the aid of guard heaters located between

the thermostat walls and regulating heaters, which were mounted inside the thermostat [61]. The pressure of the ethanol in the piezometer was measured with a dead-weight oil gauge with an estimated uncertainty of 0.05%.

The present experimental apparatus had negligible noxious volumes [58]. Taking into account the uncertainties of measurements of temperature and pressure, the combined expanded ($k = 2$) uncertainty of measuring the density was estimated to be 0.15%. The reproducibility of the data corresponding to repeated (P, T) is better than $\pm 0.1\%$. To check and confirm the accuracy of the measurements, PVT measurements were made on pure water in the critical and supercritical regions. Table I provides the present experimental PVT data for pure water measured using the same experimental apparatus. As one can see from Table I, the agreement between test measurements for pure water and IAPWS [60] formulations is good, the absolute average deviation is AAD = 0.23%. This good agreement demonstrates the reliability and accuracy of the present PVT data for pure ethanol. The commercial supplier of the methanol provided a purity analysis of 99.8 mol%.

3. RESULTS AND DISCUSSION

Measurements of the PVT properties for pure ethanol were performed in the temperature range between 373 and 673 K and at pressures from 0.226 to 40.292 MPa. The density ranged from 91.81 to

Table I. Test Measurements of the Density of Pure Water (AAD = 0.23%)

T (K)	P (MPa)	ρ ($kg \cdot m^{-3}$) [This work]	ρ ($kg \cdot m^{-3}$) IAPWS [60]	Deviations (%)
573.15	5.663	25.67	25.69	−0.08
623.15	6.417	25.61	25.59	0.08
673.15	7.124	25.55	25.52	0.12
623.15	12.890	64.93	65.20	−0.41
653.15	14.310	64.94	65.12	−0.28
673.15	15.210	64.88	65.08	−0.31
653.15	21.384	147.09	146.9	0.13
673.15	24.255	152.08	152.8	−0.47
653.15	23.534	276.62	276.0	0.22
653.15	25.227	458.02	458.7	−0.15
673.15	33.916	458.45	459.6	−0.25
653.15	26.552	488.43	490.2	−0.36
673.15	36.205	488.80	489.3	−0.10

497.67 $kg \cdot m^{-3}$. The experimental temperature, density, and pressure values for pure ethanol are presented in Table II and shown in Figs. 1–3 in P–ρ and P–T planes along the various near-critical and supercritical isotherms and quasi-isochores. These figures include also the values of PVT calculated with the fundamental equation of state by Dillon

Table II. Experimental Values of the PVT Properties of Pure Ethanol Along Near-Critical and Supercritical Isotherms

ρ ($kg \cdot m^{-3}$)	P (MPa)	ρ ($kg \cdot m^{-3}$)	P (MPa)	ρ ($kg \cdot m^{-3}$)	P (MPa)	ρ ($kg \cdot m^{-3}$)	P (MPa)
$T = 523.15$ K		$T = 573.15$ K		$T = 598.15$ K		$T = 623.15$ K	
183.48	6.896	183.03	10.531	268.76	15.360	182.58	13.905
229.90	7.053	229.90	11.753	275.40	15.638	228.74	16.019
284.72	7.241	284.72	13.124	298.43	16.553	283.27	18.927
338.77	7.505	338.77	15.106	298.42	16.550	336.99	22.541
396.85	8.198	396.85	18.056	327.82	18.187	394.68	28.485
462.15	10.95	462.15	24.481	–	–	459.51	39.211
325.46	7.450	324.61	14.445	–	–	150.13	12.169
276.57	7.206	275.87	12.868	–	–	268.41	18.031
189.75	6.922	189.28	10.658	–	–	275.04	18.476
386.40	8.029	385.36	17.431	–	–	298.03	19.706
138.64	6.564	138.30	9.119	–	–	298.03	19.708
–	–	–	–	–	–	327.39	21.748
$T = 673.15$ K		$T = 373.15$ K		$T = 423.15$ K		$T = 473.15$ K	
91.806	9.6710	271.76	0.226[a]	126.23	0.978[a]	126.23	2.978[a]
267.73	23.941	301.79	0.225[a]	196.43	0.980[a]	196.43	2.970[a]
–	–	338.61	0.227[a]	230.17	0.984[a]	230.17	2.965[a]
–	–	430.89	0.224[a]	278.12	0.985[a]	278.12	2.972[a]
–	–	–	–	306.37	0.986[a]	306.37	2.973[a]
–	–	–	–	320.42	0.988[a]	320.42	2.967[a]
–	–	–	–	334.39	0.982[a]	334.39	2.981[a]
–	–	–	–	342.30	0.987[a]	342.30	2.983[a]
–	–	–	–	386.74	0.985[a]	386.74	2.968[a]
–	–	–	–	497.67	0.983[a]	497.67	2.967[a]
$T = 548.15$ K		$T = 533.15$ K		$T = 518.15$ K		$T = 515.15$ K	
269.44	9.9710	92.420	5.899	92.487	5.417	150.922	6.189
276.09	10.080	150.79	7.290	150.90	6.379	269.899	6.288
299.20	10.400	206.81	7.819	269.85	6.630	276.556	6.289
328.67	10.959	374.71	9.601	276.51	6.642	299.713	6.302
335.71	11.212	–	–	329.18	6.752	299.706	6.303
427.14	14.904	–	–	336.23	6.781	325.597	6.322
269.44	9.9710	–	–	375.01	6.988	276.685	6.301
–	–	–	–	427.85	7.939	189.831	6.278
–	–	–	–	–	–	386.569	6.574
–	–	–	–	–	–	138.699	6.093

Table II. (continued)

ρ (kg·m^{-3})	P (MPa)	ρ (kg·m^{-3})	P (MPa)	ρ (kg·m^{-3})	P (MPa)	ρ (kg·m^{-3})	P (MPa)
$T = 503.15$ K		$T = 513.15$ K		$T = 508.15$ K		$T = 511.15$ K	
92.554	4.915	150.94	6.053	207.06	5.584[a]	269.94	5.858[a]
151.01	5.148[a]	269.92	6.085[a]	269.99	5.580[a]	276.61	5.857[a]
207.12	5.142[a]	276.58	6.086[a]	276.65	5.599[a]	–	–
270.05	5.146[a]	299.74	6.087[a]	329.35	5.583[a]	–	–
276.72	5.143[a]	329.26	6.089[a]	336.40	5.585[a]	–	–
329.43	5.147[a]	336.32	6.083[a]	375.20	5.579[a]	–	–
336.49	5.149[a]	375.10	6.118	–	–	–	–
375.29	5.149[a]	427.96	6.821	–	–	–	–
428.19	5.168[a]	–	–	–	–	–	–
$T = 493.15$ K		$T = 498.15$ K		$T = 653.15$ K		$T = 647.15$ K	
92.599	4.319[a]	270.12	4.718[a]	91.893	9.1410	205.64	16.675
207.22	4.315[a]	276.79	4.723[a]	205.58	17.126	268.09	20.369
300.04	4.317[a]	299.96	4.731[a]	274.63	21.519	274.71	20.921
–	–	329.51	4.707[a]	297.57	23.529	297.67	22.483
–	–	336.57	4.707[a]	326.88	26.102	–	–
–	–	375.39	4.716[a]	372.32	31.184	–	–
–	–	–	–	424.66	40.292	–	–
$T = 613.15$ K		$T = 553.15$ K		$T = 528.15$ K		$T = 516.15$ K	
205.98	14.190	92.33	6.528	276.37	7.801	206.98	6.364
373.12	23.812	206.60	9.526	269.71	7.760	299.70	6.425
425.61	29.869	–	–	–	–	–	–
$T = 517.15$ K		$T = 398.15$ K		$T = 512.15$ K		$T = 543.15$ K	
299.68	6.554	301.42	0.495[a]	207.02	5.954	92.376	6.211
–	–	331.11	0.497[a]	–	–	–	–
$T = 563.15$ K		$T = 618.15$ K		$T = 638.15$ K		$T = 521.15$ K	
92.288	6.805	92.046	8.359	91.959	8.910	206.93	6.800
$T = 583.15$ K		–	–	–	–	–	–
206.29	11.872	–	–	–	–	–	–

[a] Two-phase values

and Penoncello [46] and the data reported by other authors (Fig. 3). The experimental and calculated values of the compressibility factor $Z = PV/(RT)$ as a function of pressure P are given in Fig. 4. This figure demonstrates the good mutual consistency of the measured values of temperature T, pressure P, and specific volume V for each thermodynamic state (P, V, T) and the results of calculations using the Dillon and Penoncello [46] equation of state. Figure 5 shows the measured values of PVT in the two-phase region (sub-critical region, along the sub-critical isotherms). In order to determine the values of saturated densities and

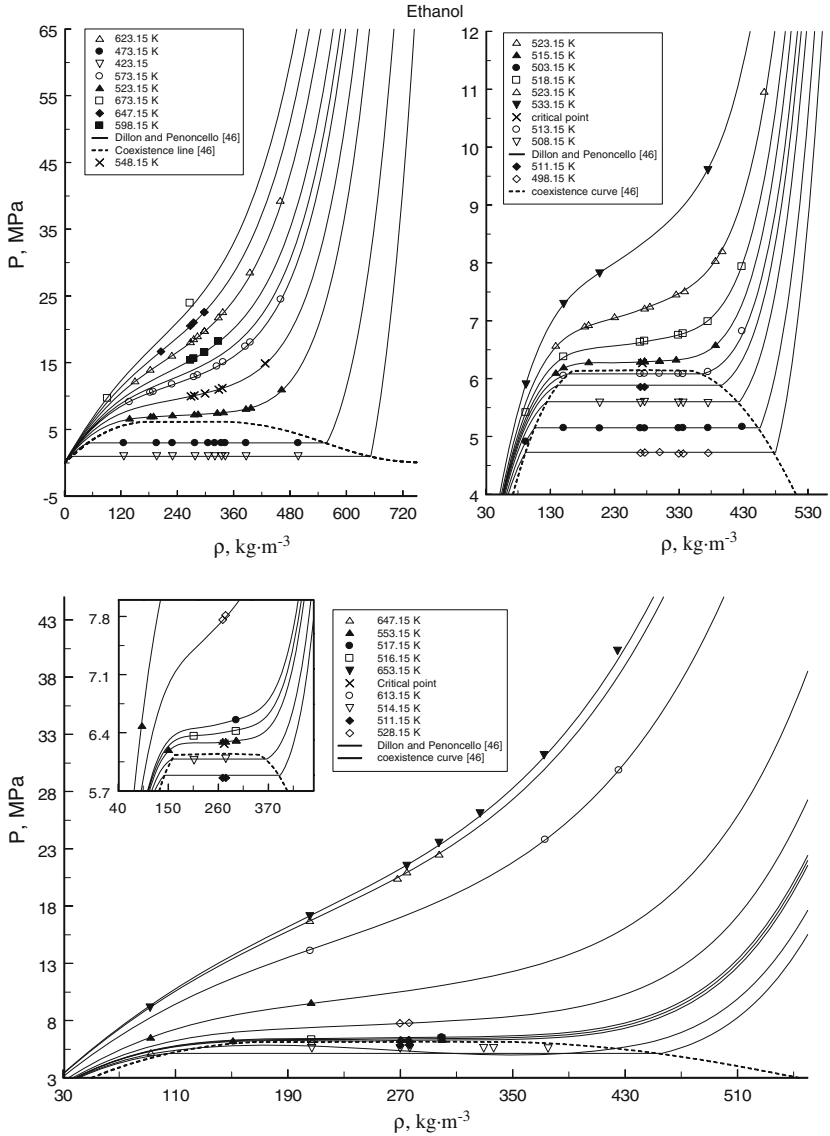

Fig. 1. Measured values of pressure of ethanol as a function of density along the various near- and supercritical isotherms together with values calculated from the Dillon and Penoncello [46] fundamental equation of state.

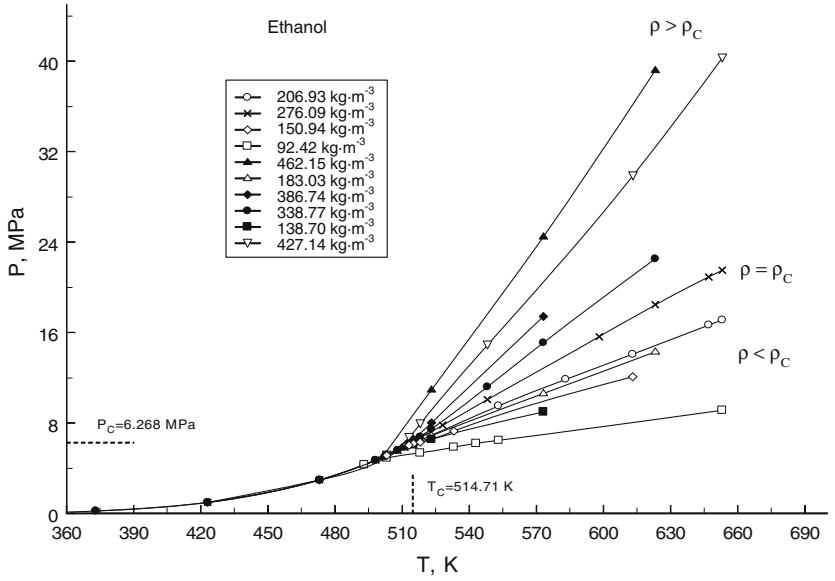

Fig. 2. Measured values of pressure of ethanol as a function of temperature along the various near-critical isochores together with values calculated from the Dillon and Penoncello [46] fundamental equation of state.

pressures, the two-phase experimental isotherms were analytically extrapolated to the vapor-pressure curve. Figure 6 demonstrates also the isothermal break-point technique to determine values of the saturated property from *P–T* measurements in the two- and one-phase regions. The saturation properties were determined as the intersection of the two-phase and one-phase *P–T* curves (see Fig. 6). The saturated-liquid and -vapor densities and vapor-pressure data extracted from these two-phase *PVT* measurements are summarized in Table III and presented in Figs. 7 and 8 together with reported data and values calculated with the Dillon and Penoncello [46] equation of state and correlations by other authors.

3.1. Comparisons with Other Data

The *PVT* data of ethanol measured in this work were compared with values reported by other authors. Detailed direct comparisons of the present *PVT* data with the equation of state (EOS) by Dillon and Penoncello [46] and other reported data are shows in Figs. 1–4. The deviations between the present measured densities and the values calculated from Dillon and Penoncello [46] EOS are given in Fig. 9 as a function of pressure

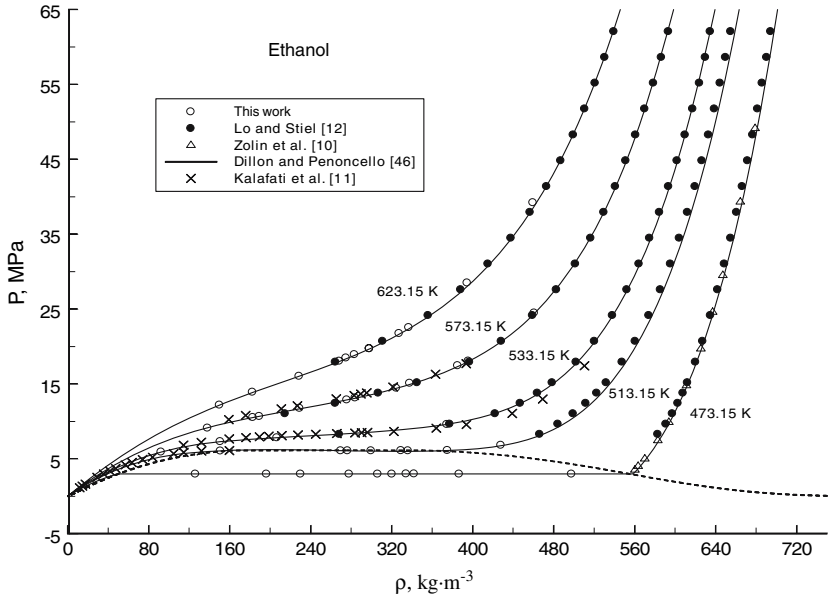

Fig. 3. Comparison of the present experimental pressures for ethanol with data reported by other authors and calculated from the Dillon and Penoncello [46] fundamental equation of state.

for various measured isotherms. The agreement between the present data and the values of density calculated with the Dillon and Penoncello [46] EOS is satisfactory (AAD = 0.49%, Bias = 0.069%, St.Dev. = 0.58%, St.Err. = 0.067%) in the temperature range below 650 K where the EOS is applicable. Extrapolated to higher temperatures (out of the range of validity of the EOS, above 650 K), the values of density calculated with the EOS deviate from the present data within 2.19% with a maximum deviation of 5%. In the immediate vicinity of the critical point (within $T_C \pm 3$ K), the discrepancy between the measured and calculated values of density varies from 2.3 to 2.7%. The deviations between measured and calculated values of pressure are within 0.3% at low temperatures, while at high temperatures the deviations increase to 2%, and in the extrapolation range (above 650 K), the deviations are about 3–5%.

Detailed comparisons between the present data for vapor pressure and saturated density and the results reported by other authors and calculated with various correlations are presented in Tables IV–VI. As one can see from these tables, the majority of the reported and correlated data deviate from the present values of vapor pressure within 0.33–0.61%. Good agreement with an AAD = 0.4% is found between the present data

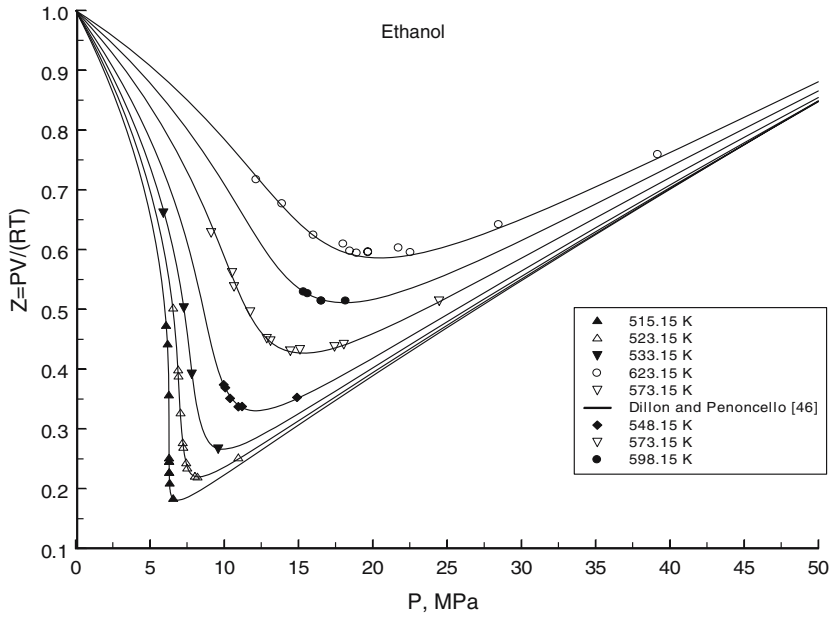

Fig. 4. Compressibility factors, $Z = PV/(RT)$, of the ethanol as a function of pressure P along the supercritical isotherms together with values calculated with the Dillon and Penoncello [46] equation of state.

and the values calculated from the EOS of Dillon and Penoncello [46]. Good agreement within 0.33% is also found between the present data and those reported by Deák et al. [16]. Large differences up to 2.16 and 5.0% are found for the vapor pressures reported by Zolin et al. [10] and Mousa [27], respectively.

Details of comparisons between the present saturated-liquid and -vapor-density data and results reported by other authors and calculated with various correlations are given in Tables V and VI. Basically the agreement between the present data and the most reliable reported results from the literature is good, except for the data reported by Mousa [27] (AAD = 14%) and the data by Skaates and Kay [21] (AAD = 3.42%). These tables show that our data are consistent with most reported values. Excellent agreement with AADs of 0.09, 0.13, and 0.25% is observed between the present measurements and the values of saturated-liquid densities reported by Sauermann et al. [13] and calculated from the EOS by Dillon and Penoncello [46] and correlation of Hales and Ellender [32], respectively. The measurements by Costello and Bowden [36] deviate from the present values within 0.23%. The data of Zolin et al. [10] and the

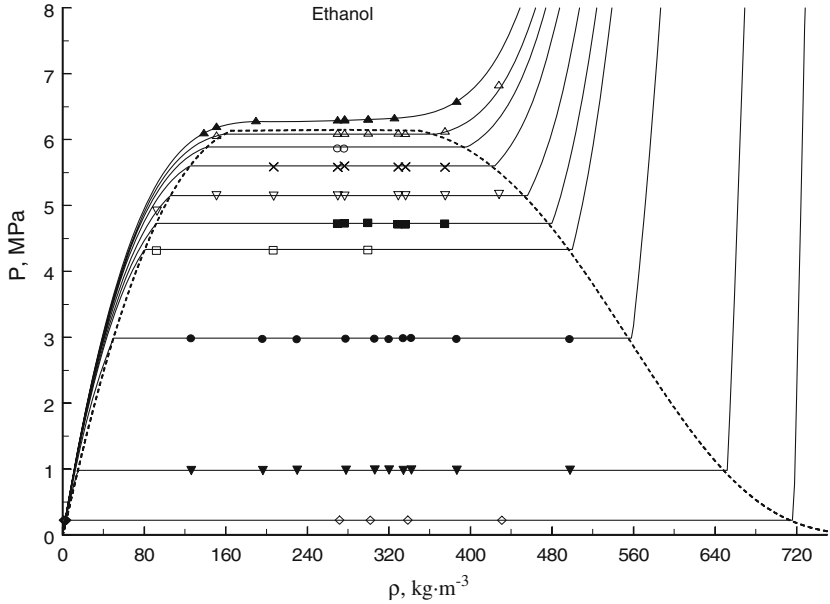

Fig. 5. Measured values of pressure of ethanol as a function of density along the various near-sub-critical isotherms together with values calculated with the Dillon and Penoncello [46] fundamental equation of state. ◇, 373.15 K; ▼, 423.15 K; •, 473.15 K; □, 493.15 K; ■, 498.15 K; ∇, 503.15 K; ×, 508.15 K; ◯, 511.15 K; Δ, 513.15 K; ▲, 515.15 K; (—), Dillon and Penoncello [46]; (– – – –), coexistence curve [46].

correlation by Cibulka [47] show deviations within 0.89% and 0.80%, respectively. The saturated temperature data in the critical region reported by Gasanov [39] are systematically higher (by 7–8 K) than the present and other published data. Relatively large deviations are found between the present measurements of saturated-vapor densities and reported data and correlations. The values of saturated-vapor density calculated with the EOS by Dillon and Penoncello [46] deviate from the present data within 0.58%, while the data of Mousa [27] and Skaates and Kay [21] show deviations up to 13.9 and 22%, respectively. The measurements by Costello and Bowden [36] for the saturated vapor-density deviate from the present data within 2.8%.

The shape of the coexistence curve in the critical region for ethanol reported by various authors from the literature together with the present results is depicted in Fig. 10. This figure contains also the values of saturated densities derived in our calorimetric experiments [37] in the critical region. A large scatter (up to 10 K for the saturated temperature and 50% for the saturated density) of the various data sets and correlations is

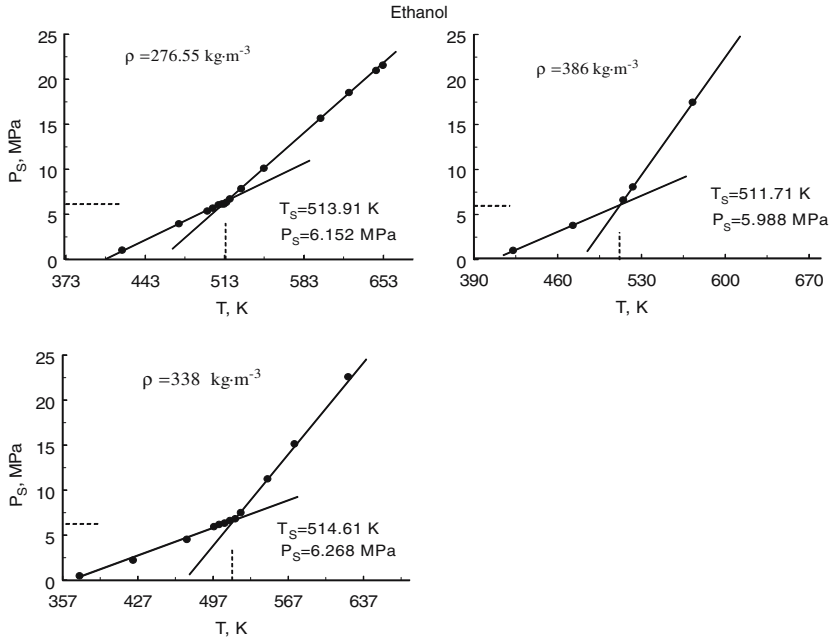

Fig. 6. Intercept (isochoric break points) of the two- and one-phase isochores for ethanol.

observed near the critical point (see Fig. 10). The same character of deviations is found also for the reported critical temperatures and the critical densities (see Section 3.2). As one can see from this figure, the most probable values of the critical temperature and critical density of ethanol lie between 514.0 and 514.7 K and between 273 and 283 $\mathrm{kg \cdot m^{-3}}$, respectively. Probably this relatively large range is due to impurity and thermal decomposition effects on the measured properties at high temperatures.

3.2. Critical Parameter Determination

The derived values of the saturated densities and pressure near the critical point were used to estimate the critical parameters for pure ethanol. Figure 11 shows the density differences (saturated-liquid and -vapor densities), $\Delta\rho_S = \rho'_S - \rho''_S$, at saturation as a function of temperature in the critical region. This figure also includes the measured data for $\Delta\rho_S$ reported by Costello and Bowden [36] and by Young [73]. The fitting procedure was used to calculate the values of the critical parameters (T_C and ρ_C) for ethanol. In order to estimate the value of the critical temperature, the values of $\Delta\rho_S = \rho'_S - \rho''_S$ were analytically extrapolated to zero

Table III. Temperatures, Pressures, and Densities at Saturation for Pure Ethanol

T_S (K)	P_S (MPa)	ρ'_S (kg·m^{-3})	ρ''_S (kg·m^{-3})
373.15	0.226	712.93	3.7500
398.15	0.498	–	–
423.15	0.983	647.87	15.230
473.15	2.945	555.23	50.010
493.15	4.315	495.58	80.510
498.15	4.715	476.56	91.690
503.15	5.145	453.07	104.99
508.15	5.583	420.33	124.47
511.15	5.860	392.86	140.95
512.15	5.954	–	–
513.15	6.085	361.08	160.00

($\Delta\rho_S \to 0$, where the densities of the liquid and vapor become identical) using a scaling-type equation (see below). The optimal value of the temperature when $\Delta\rho_S = 0$ (where the difference between the liquid and vapor

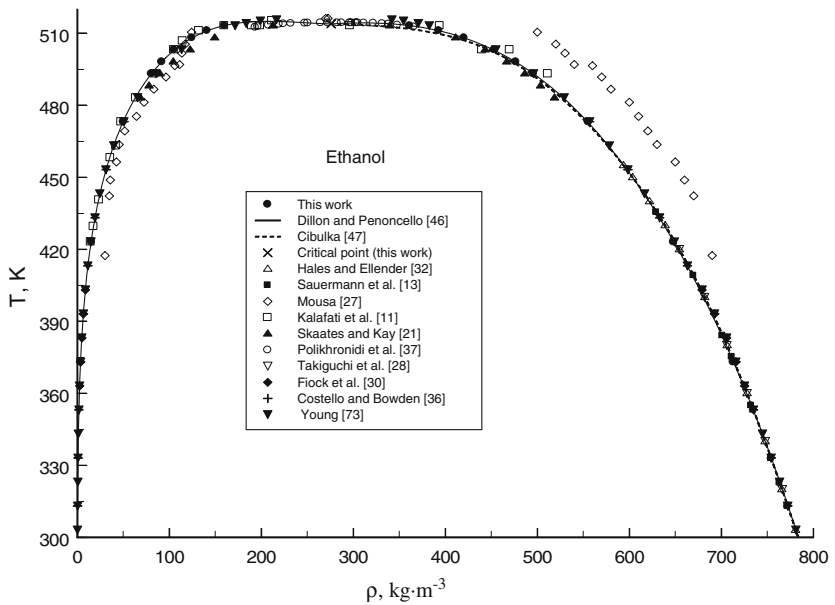

Fig. 7. Comparisons of the present saturated-liquid and -vapor densities for ethanol with data reported by other authors from the literature and calculated with various correlations.

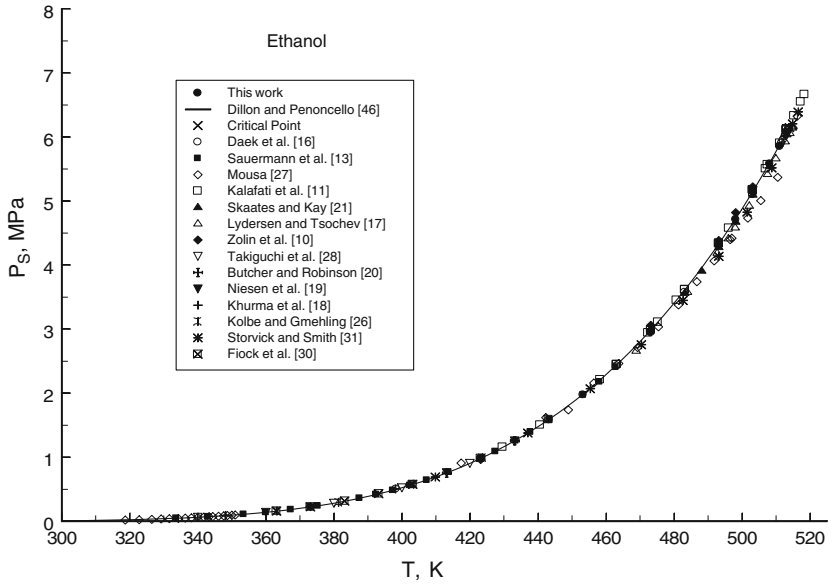

Fig. 8. Comparisons of the present vapor pressures for ethanol with data reported by various authors and calculated with the Dillon and Penoncello [46] fundamental equation of state.

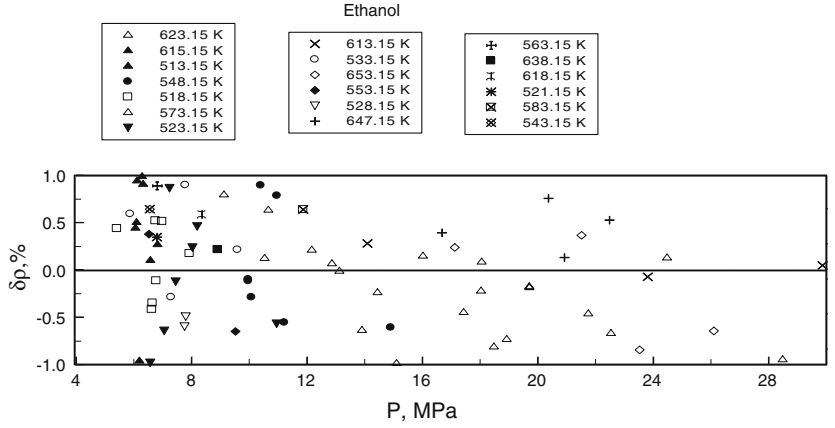

Fig. 9. Percentage deviations, $\delta\rho = 100\left(\frac{\rho^{\exp}-\rho^{\mathrm{cal}}}{\rho^{\exp}}\right)$ of the present experimental densities for ethanol from values calculated with the Dillon and Penoncello [46] fundamental equation of state.

Table IV. Comparison of Vapor-Pressure (MPa) Measurements of Ethanol with Selected Literature Values

T_S (K)	This work	Ambrose et al. [22–25]	Dillon and Penoncello [46]	Kalafati et al. [11][a]	Lydersen and Tsochev [17]	Mousa [27]	Sauermann et al. [13]	Deák et al. [16]	Skaates and Kay [21]	Zolin et al. [10]
373.15	0.226	0.2237	0.2253	–	0.2405[a]	0.2339	0.2251	–	–	0.230
398.15	0.498	0.5012	0.4969	–	0.5037[a]	0.6759	0.4973	–	–	0.572
423.15	0.983	0.9788	0.9823	0.984	0.9667[a]	1.0365	0.9795	0.981	–	0.965
473.15	2.945	2.9573	2.9871	2.987	2.9220[a]	2.9696	2.9535	2.963	–	3.060
493.15	4.315	4.2888	4.3323	4.333	4.2241	4.1579	4.2821	4.343	4.2775	4.385
498.15	4.715	4.6845	4.7291	4.751	4.6145	4.4955	4.6776	4.727	4.6760	4.822
503.15	5.145	5.1086	5.1523	5.180	5.0372	4.8496	5.1022	5.106	5.0980	5.224
508.15	5.573	5.5636	5.6034	5.620	5.4891	5.2203	5.5586	5.576	5.5500	–
511.15	5.860	5.8527	5.8884	5.906	5.7748	5.4507	5.8493	5.860	5.8430	–
512.15	5.954	5.9528	5.9859	6.100	5.9284	5.6486	5.9502	5.965	5.9407	–
513.15	6.085	6.0530	6.0847	6.110	5.9715	5.6077	6.0511	6.070	6.0405	–
AAD (%)	0.0	0.48	0.40	0.87	1.55	5.00	0.42	0.33	0.61	2.16

T_S (K)	This work	Kolbe and Gmehling [26]	Niesen et al. [19]	Butcher and Robinson [20]	Takiguchi et al. [28]	Khurma et al. [18]	Fiock et al. [30]	Storvick and Smith [31]	
373.15	0.226	0.233[a]	–	–	0.234[a]	0.229[a]	0.226[a]	–	–
398.15	0.498	0.510[a]	–	–	0.502[a]	0.501[a]	0.503[a]	–	–
423.15	0.983	0.982[a]	1.007[a]	1.009[a]	–	–	–	1.029[a]	–
473.15	2.945	–	–	–	–	–	–	2.916[a]	–
493.15	4.315	–	–	–	–	–	–	4.137	–
498.15	4.715	–	–	–	–	–	–	4.551[a]	–
503.15	5.145	–		–	–	–	–	4.986[a]	–
508.15	5.573	–	–	–	–	–	–	5.516[a]	–
511.15	5.860	–	–	–	–	–	–	–	–
512.15	5.954	–	–	–	–	–	–	–	–
513.15	6.085	–	–	–	–	–	–	–	–
AAD (%)	0.0	1.86	1.01	1.01	2.50	0.95	0.5	2.93	–

[a] Analytically interpolated values.

Table V. Comparison of Saturated-Liquid-Density ($kg \cdot m^{-3}$) Measurements of Ethanol with Selected Literature Values

T_S (K)	This work	Cibulka [47]	Dillon and Penoncello [46]	Costello and Bowden [36]	Zolin et al. [10]	Mousa [27]	Hales and Ellender [32]	Skaates and Kay [21]	Sauermann et al. [13]	Takiguchi et al. [28]	Fiock et al. [30]
373.15	712.93	713.85	713.14	715.7	714.35	–	713.82	–	713.55	713.46	715.82
423.15	647.87	649.52	648.27	648.0	650.15	685.38	649.54	–	648.52	–	–
473.15	555.23	552.86	554.66	556.8	553.72	613.69	553.04	–	–	–	–
493.15	495.58	493.62	496.07	–	490.14	572.87	496.00	486.3	–	–	–
498.15	476.56	472.71	476.24	–	470.19	537.87	478.30	466.8	–	–	–
503.15	453.07	447.28	452.12	–	444.06	526.18	457.93	443.2	–	–	–
508.15	420.33	410.54	420.15	–	416.28	509.40	432.14	411.3	–	–	–
511.15	392.86	–	392.57	–	–	473.77	409.03	368.2	–	–	–
513.15	361.08	–	362.84	–	–	393.07	377.30	339.5	–	–	–
AAD (%)	0.0	0.80	0.13	0.23	0.89	13.9	0.25	3.42	0.09	0.07	0.40

Table VI. Comparison of Saturated-Vapor-Density Measurements of Ethanol with Selected Literature Values

T_S (K)	This work	Dillon and Penoncello [46]	Kalafati et al. [11]	Mousa [27]	Skaates and Kay [21]	Fiock et al. [30]	Costello and Bowden [36]
373.15	3.7500	3.5300	–	–	–	3.602	3.602
423.15	15.230	14.973	14.580	31.180	–	–	–
473.15	50.010	49.801	47.664	59.580	–	–	50.8
493.15	80.510	80.488	–	99.110	89.70	–	–
498.15	91.690	91.770	–	111.79	104.3	–	–
503.15	104.99	105.85	–	114.97	122.6	–	–
508.15	124.47	124.96	–	120.96	149.3	–	–
511.15	140.95	141.68	–	141.21	187.3	–	–
513.15	160.00	158.84	–	193.25	212.6	–	–
AAD (%)	0.0	0.58		13.90	21.70	4.1	2.8

phases vanishes), was accepted as the critical temperature for ethanol. The derived value of the critical temperature is 514.71 ± 0.2 K. Because the isothermal compressibility of the fluid is infinite ($K_T \to +\infty$) at the critical point, it is difficult to accurately measure the critical density directly. To calculate the value of the critical density ρ_C the values of the saturated density ρ_S were fitted to the "complete scaling" relation [62,63],

$$\Delta\rho = \pm B_0 t^{\beta} \pm B_1 t^{\beta+\Delta} + B_2 t^{1-\alpha} - B_3 t + B_4 t^{2\beta}, \tag{1}$$

where $\Delta\rho = (\rho - \rho_C)/\rho_C$; ρ_C is the critical density (considered as an adjustable parameter); $t = (T_C - T)/T_C$; $T_C = 514.71 \pm 0.2$ K (the critical temperature is derived as described above); $\beta = 0.324$, $\alpha = 0.11$, and $\Delta = 0.51$ are the universal critical exponents; and $B_i (i = 0, 4)$ are the adjustable critical amplitudes. A Yang–Yang anomaly of strength $R_\mu = A_\mu/(A_P + A_\mu)$ effect on the coexistence curve diameter is given by [62,63]

$$\rho_d = 1 + \left(B_2 t^{1-\alpha} - B_3 t + B_4 t^{2\beta} \right), \tag{2}$$

where $\rho_d = \left(\rho'_S + \rho''_S\right)/2\rho_C$ is the reduced coexistence curve diameter; $B_4 \propto A_\mu/A_P$, where A_μ, A_P are the critical amplitudes of second temperature derivatives of vapor-pressure curve, (d^2P/dT^2), and chemical potential, $(d^2\mu/dT^2)$, respectively. A Yang–Yang anomaly ($d^2\mu/dT^2 \to \pm\infty$) implies a leading correction $\rho_d \propto B_4 t^{2\beta}$ would dominate the previously expected $\rho_d \propto B_2 t^{1-\alpha}$ correction [62,63]. In Eq. (1), $\pm B_0 t^{\beta}$ is the asymptotic (symmetric) term, $\pm B_1 t^{\beta+\Delta}$ is the nonasymptotic (symmetric Wegner's

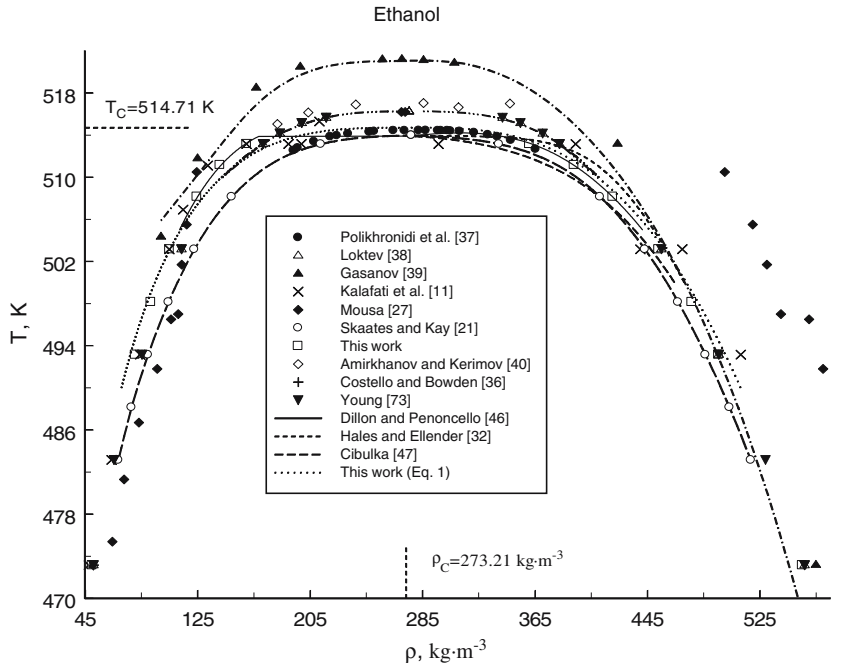

Fig. 10. Shape of the coexistence curve for ethanol near the critical point reported by various authors from the literature and calculated with various correlations.

correction) term; $B_2 t^{1-\alpha}$ is the "singular diameter" the first nonanalytical contribution to liquid-gas asymmetry; $B_4 t^{2\beta}$ is the new nonanalytical contribution of liquid-gas asymmetry ("complete scaling" term), and $B_3 t$ is the rectilinear diameter. According to the theory of "complete scaling" (Eq. (1)), the first temperature derivative of the coexistence-curve diameter diverges as the isochoric heat capacity $(d\rho_d/dT) \propto t^{-\alpha}$ and as $(d\rho_d/dT) \propto t^{2\beta-1}$ $(2\beta - 1 \approx -0.352)$, i.e., the divergence is shared among the two terms, $B_2 t^{1-\alpha}$ and $B_4 t^{2\beta}$. We accurately determined the critical amplitudes B_2 and B_4 from the present experimental data for ethanol (see Table VII), i.e., the singular contribution of both terms. Figure 12 demonstrates that both $(B_2 t^{1-\alpha})$ and $(B_4 t^{2\beta})$ represent nonanalytical contributions of the singular diameter of ethanol. If we define the strength of the coexistence curve diameter singularity as $B_\mu = B_4/(B_4 + B_2)$, like the Yang–Yang anomaly of strength $R_\mu = A_\mu/(A_P + A_\mu)$, then at $B_\mu = 0$, therefore, $B_4 = 0$, the divergence of the coexistence curve diameter, $d\rho_d/d\tau$, is caused by divergence of only the $B_2 t^{1-\alpha}$ term in Eq. (1). However, if $B_\mu \neq 0$, i.e., $B_4 \neq 0$, the divergence of the coexistence curve diameter, $d\rho_d/d\tau$, is caused

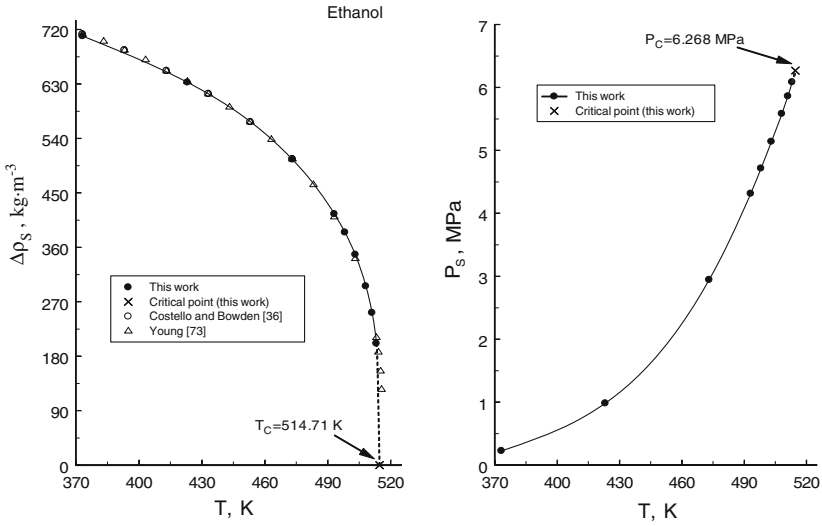

Fig. 11. Saturated-liquid and -vapor density differences, $\Delta\rho_S = \rho'_S - \rho''_S$, and vapor pressure of the ethanol near the critical point.

by divergence of both $B_2 t^{1-\alpha}$ and $B_4 t^{2\beta}$ terms in Eq. (1). As one can see from Table VII, the value of $B_4 \neq 0$; therefore, $B_\mu \neq 0$ ($B_\mu = 0.13$ for ethanol). For ethanol, the value of the critical amplitude B_4 ($B_4 t^{2\beta}$) is small and negative (-0.9442), while the value of the critical amplitude B_2 is large and positive (6.2812). Therefore, both nonanalytical contributions to the singular diameter of ethanol partially compensate each other, and as previously shown by Anisimov and Wang [64], create an illusion that the diameter is rectilinear (see Fig. 12). Thus, the present experimental data for the coexistence curve diameter exhibit slight deviations from the straight lines (rectilinearity). As shown previously by Anisimov and Wang [64], for some fluids (for example, SF_6, n-C_7H_{16}) the term $B_4 t^{2\beta}$ is dominant, while for other fluids such as Ne, N_2, and CH_4, the contribution of the $B_4 t^{2\beta}$ term is negative and small, such as our case for ethanol. Thus, the divergence of the coexistence curve diameter, $d\rho_d/d\tau$, for ethanol is shared between the terms $B_2 t^{1-\alpha}$ and $B_4 t^{2\beta}$; moreover, the contribution of the $B_2 t^{1-\alpha}$ term is dominant, although for some fluids depending on the effect of their nature on coexistence curve asymmetry, the domination of the $B_4 t^{2\beta}$ is possible (see, for example, Ref. 64).

Usually, the value of the critical density determined from the singular diameter law is less than that obtained from the linear extrapolation (from rectilinear law). In some cases the resulting difference between "rectilinear"

Table VII. Coefficients B_i and P_i for Eqs. (1) and (3)

B_0	B_1	B_2	B_3	B_4	Thermodynamic path
2.2992	−0.6732	6.2812	4.6700	−0.9442	Along the coexistence curve
P_1	P_2	P_3	–	–	Thermodynamic path
183.6693	−146.3741	−56.1697	–	–	Vapor-pressure curve

$T_C = 514.71 \pm 0.2\,\mathrm{K}$, $\rho_C = 273.21 \pm 2\,\mathrm{kg \cdot m^{-3}}$, $P_C = 6.268 \pm 0.008\,\mathrm{MPa}$; $\alpha = 0.11$; $\beta = 0.324$; $\Delta = 0.51$

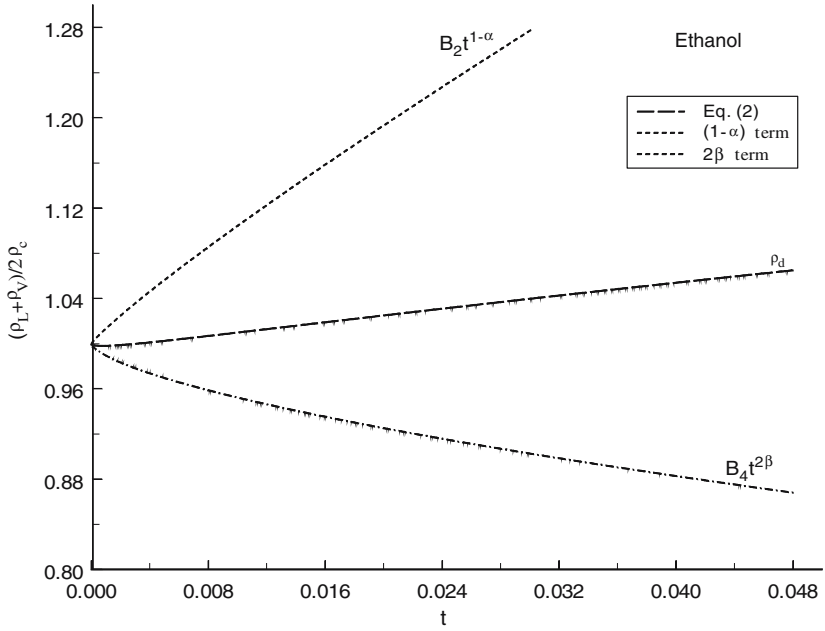

Fig. 12. Singular diameters for ethanol.

and "singular" diameter techniques for the critical density determination is about 3–5%. For ethanol most available data for the critical density differ by $\pm 2\,\mathrm{kg \cdot m^{-3}}$ (or about 1%). This is indirectly confirming that the diameter of the ethanol is close to rectilinear. The derived optimal value of $\rho_C = 273.21 \pm 2\,\mathrm{kg \cdot m^{-3}}$ was accepted as the critical density for ethanol.

The present saturated-pressure values were analytically extrapolated, by using the scaling relation near the critical point,

$$P_S = P_C + P_1 t^{2-\alpha} + P_2 t^{2-\alpha+\Delta} + P_3 t \tag{3}$$

to the value of the derived critical temperature ($T_C = 514.71$ K) (see Fig. 11b). The derived value of the critical pressure for ethanol is $P_C = 6.268 \pm 0.008$ MPa. The values of the adjustable parameters of Eq. (3) are given in Table VII. The present derived values of the critical parameters for pure ethanol ($T_C = 514.71 \pm 0.2$ K, $\rho_C = 273.21 \pm 2\,\mathrm{kg \cdot m^{-3}}$, $P_C = 6.268 \pm 0.008$ MPa) are in satisfactory agreement with the most reliable reported values. Differences between the critical temperature, density, and pressure recommended by Gude and Teja [48] and the present results are 0.71 K, 0.65, and 2.1%, respectively. Dillon and Penoncello [46] recommended values of the critical parameters that deviate from the present data by 0.81 K, 1.0, and 1.95%, respectively. Our recent calorimetric measurement results for the critical parameters (T_C and ρ_C) deviate from the present PVT experimental results within 0.27 K and 3.3%. The present results for the critical parameters are also good (0.2–0.6 K, 0.02–0.08 MPa, and 2–3 $\mathrm{kg \cdot m^{-3}}$), based on comparisons with data reported by other authors [17, 22, 32, 65–73]. Large differences (up to 2–3 K , for the critical temperature) were found for data reported by other authors [17, 31, 36, 74–82] and (10–45 $\mathrm{kg \cdot m^{-3}}$ for the critical density) were found for data reported by Polikhronidi et al. [37], Battelli [66], and Ramsay and Young [77].

4. CONCLUSIONS

Densities of pure ethanol along 33 near-critical and supercritical isotherms between 373 and 673 K and at pressures from 0.226 to 40.292 MPa have been measured with a constant-volume piezometer technique. The density ranged from 91.81 to 497.67 $\mathrm{kg \cdot m^{-3}}$. The measured values of PVT in the two- and one-phase regions were used to accurately determine the values of the vapor pressure and saturated-liquid and -vapor densities in the temperature range from 373 to 513 K by using analytical extrapolation and the break-point technique. The critical parameters ($T_C = 514.71 \pm 0.2$ K, $\rho_C = 273.21 \pm 2\,\mathrm{kg \cdot m^{-3}}$, $P_C = 6.268 \pm 0.008$ MPa) for pure ethanol were determined from measured values of saturation properties using a fitting procedure. The measured PVT data and saturated properties are in good agreement (AAD = 0.49%) with values calculated from the fundamental equation of state by Dillon and Penoncello [46]. Large discrepancies (up to 10 K and 50%) were found between various reported saturated- and critical-properties data for ethanol in the critical region. Derived values of the saturation densities and vapor pressure were used to develop scaling-type correlation equations in the critical region. The singularity of the coexistence-curve diameter is caused by divergence of both $B_2 t^{1-\alpha}$ and $B_4 t^{2\beta}$ terms in the "complete scaling" equation. For ethanol

the value of the coexistence-diameter singularity strength defined as B_μ is not zero. But, both nonanalytical contributions, $B_2 t^{1-\alpha}$ and $B_4 t^{2\beta}$, of the singular diameter partially compensate each other (the coefficients B_2 and B_4 have opposite signs), and the diameter of ethanol is very close to rectilinear.

ACKNOWLEDGMENTS

One of us, I.M.A., thanks the Physical and Chemical Properties Division at the National Institute of Standards and Technology for the opportunity to work as a Guest Researcher at NIST during the course of this research. We also thank Dr. G. Rabadanov for the chromatography analysis of the methanol sample before and after experiments.

REFERENCES

1. M. Budich and G. Brunner, *J. Supercrit. Fluids* **25**:45 (2003).
2. J. S. Lim and Y. Y. Lee, *J. Supercrit. Fluids* **7**:219 (1994).
3. N. Ikawa, Y. Nagase, T. Tada, S. Furuta, and R. Fukuzato, *Fluid Phase Equilib.* **83**:167 (1993).
4. R. Fukuzato, N. Ikawa, and Y. Nagase, in *Value Adding through Solvent Extraction*, D. C. Shallcross, R. Painmin, and L. M. Prvcic, eds. (University of Melbourne, Australia, 1996), Vol. 2, p. 1011.
5. S. Hirohama, T. Takatsuka, S. Miyamoto, and T. Muto, *J. Chem. Eng. Jpn.* **26**:243 (1993).
6. S. Furuta, N. Ikawa, R. Furuzato, and N. Imanishi, *Kagaku Kogaku Ronbunshu* **15**:519 (1989).
7. J. Schanzenbacher, J. D. Taylor, and J. W. Tester, *J. Supercrit. Fluids* **22**:139 (2002).
8. O. J. Catchpole, N. B. Perry, B. M. T. de Silva, J. B. Grey, and B. M. Smallfield, *J. Supercrit. Fluids* **22**:129 (2002).
9. I. F. Golubev, T. N. Vasil'kovskaya, and V. S. Zolin, *Inzh.-Fiz. Zh.* **38**:668 (1980).
10. V. S. Zolin, T. N. Vasil'kovskaya, and I. F. Golubev, *Thermophys. Prop. Subst. Mater.* **18**:20 (1983).
11. D. D. Kalafati, D. S. Rasskazov, and E. K. Petrov, *Teploenergetika* **14**:77 (1967).
12. H. Y. Lo and L. I. Stiel, *Ind. Eng. Chem. Fund.* **8**:713 (1969).
13. P. Sauermann, K. Holzapfel, J. Oprzynski, F. Kohler, W. Poot, and Th. W. de Loos, *Fluid Phase Equilib.* **112**:249 (1995).
14. V. G. Tamman and A. Rühenbeck, *Ann. Phys.* **13**:63 (1932).
15. V. N. Popov and B. A. Malov , *Trud. Moscow Power Eng. Institute* (Moscow, MEI, 1971), pp. 2–11.
16. A. Deák, A. I. Victorov, and Th. W. de Loos, *Fluid Phase Equilib.* **107**:277 (1995).
17. A. L. Lydersen and V. Tsochev, *Chem. Eng. Technol.* **13**:125 (1990).
18. J. R. Khurma, O. Muthu, S. Munjal, and B. D. Smith, *J. Chem. Eng. Data* **28**:100 (1983).
19. V. Niesen, A. M. F. Palavre, A. J. Kidney, and V. F. Yesavage, *Fluid Phase Equilib.* **31**:283 (1986).
20. K. L. Butcher and W. I. Robinson, *J. Appl. Chem*. **16**:289 (1966).
21. J. M. Skaates and W. B. Kay, *Chem. Eng. Sci.* **19**:431 (1964).

22. D. Ambrose and J. Walton, *Pure Appl. Chem.* **61**:1395 (1989).
23. D. Ambrose and C. H. S. Sprake, *J. Chem. Thermodyn.* **2**:631 (1970).
24. D. Ambrose, J. H. Ellender, and C. H. S. Sprake, *J. Chem. Thermodyn.* **6**:909 (1974).
25. D. Ambrose, C. H. S. Sprake, and R. Townsend, *J. Chem. Thermodyn.* **7**:185 (1975).
26. B. Kolbe and J. Gmehling, *Fluid Phase Equilib.* **23**:213 (1985).
27. A. H. N. Mousa, *J. Chem. Eng. Jap.* **20**:635 (1987).
28. Y. Takiguchi, M. Kamiya, and M. Uematsu, *Nippon Kikai Gakkai Ronbunshu B Hen* **61**:644 (1995).
29. B. D. Smith and R. Srivastava, *Thermodynamic Data for Pure Compounds* (Elsevier, Amsterdam, 1986).
30. E. Fiock, D. C. Ginnings, and W. B. Holton, *J. Res. Nat. Bur. Stand.* **6**:881 (1931).
31. T. S. Storvick and J. M. Smith, *J. Chem. Eng. Data* **5**:133 (1960).
32. J. L. Hales and J. H. Ellender, *J. Chem. Thermodyn.* **8**:1177 (1976).
33. V. F. Nozdrev, *Ultrasonic technique in molecular physics* (Moscow, Nauka, 1958).
34. Y. Takiguchi and M. Uematsu, *Int. J. Thermophys.* **16**:205 (1995).
35. Y. Takiguchi and M. Uematsu, *J. Chem. Thermodyn.* **28**:7 (1996).
36. J. M. Costello and S. T. Bowden, *Rec. Trav. Chim. Pays-Bas* **77**:36 (1958)
37. N. G. Polikhronidi, I. M. Abdulagatov, G. V. Stepanov, and R. G. Batyrova *J. Supercrit. Fluids* (2007), submitted.
38. S. M. Loktev, *High Fat Alcohols* (Khimiya, Moscow, 1970).
39. N. S. Gasanov, *Ph. D. Thesis* (Dushanbe, 1972).
40. Kh. I. Amirkhanov and A. M. Kerimov, *Russ. J. Phys. Chem.* **32**:1697 (1958).
41. A. M. Kerimov, M. K. Alieva, and N. S. Gasanov, *Izv. AN Azerb. Ser. Phys. & Math.* **4**:149 (1971).
42. H. Kitajima, N. Kagawa, S. Tsuruno, and H. Endo, *Trans. Jpn. Soc. Mech. Eng. Ser. B* **69**:1921 (2003).
43. K. G. Akhmetzyanov, *Vest. Moscovskogo Universiteta* **6**:93 (1949)
44. M. D. Vine and C. J. Wormald , *J. Chem. Thermodyn.* **21**:1151 (1989).
45. M. Radosz and A. Lydersen, *Chem. Ing. Tech*. **52**:756 (1980).
46. H. E. Dillon and S. G. Penoncello, *Int. J. Thermophys.* **25**:321 (2004).
47. I. Cibulka, *Fluid Phase Equilib.* **89**:1 (1993).
48. M. Gude and A. S. Teja, *J. Chem. Eng. Data* **40**:1025 (1995).
49. I. M. Abdulagatov, A. R. Bazaev, and A. E. Ramazanova, *Int. J. Thermophys.* **14**:231 (1993).
50. I. M. Abdulagatov, A. R. Bazaev, E. A. Bazaev, M. B. Saidakhmedova, and A. E. Ramazanova, *J. Chem. Eng. Data* **43**:451 (1998).
51. I. M. Abdulagatov, A. R. Bazaev, E. A. Bazaev, M. B. Saidakhmedova, and A. E. Ramazanova, *Fluid Phase Equilib.* **150**:537 (1998).
52. I. M. Abdulagatov, A. R. Bazaev, E. A. Bazaev, and M. G. Rabezkii, *J. Supercrit. Fluids* **19**:219 (2001).
53. I. M. Abdulagatov, A. R. Bazaev, J. W. Magee, S. B. Kiselev, and J. F. Ely, *Ind. Eng. Chem. Res.* **44**:1967 (2005).
54. A. R. Bazaev, I. M. Abdulagatov, E. A. Bazaev, A. A. Abdurashidova, and A. E. Ramazanova, *J. Supercrit. Fluids* (in press).
55. A. R. Bazaev, I. M. Abdulagatov, J. W. Magee, E. A. Bazaev, and M. G. Rabezkii, *J. Chem. Eng. Data* **46**:1089 (2001).
56. A. R. Bazaev, I. M. Abdulagatov, J. W. Magee, E. A. Bazaev, and A. E. Ramazanova, *J. Supercrit. Fluids* **26**:115 (2003).
57. A. R. Bazaev, I. M. Abdulagatov, J. W. Magee, E. A. Bazaev, A. E. Ramazanova, and A. A. Abdurashidova, *Int. J. Thermophys.* **25**:804 (2004).

58. A. R. Bazaev, I. M. Abdulagatov, E. A. Bazaev, and A. A. Abdurashidova, *J. Chem. Thermodyn.* **39**:385 (2007).
59. M. G. Rabezkii, A. R. Bazaev, I. M. Abdulagatov, J. W. Magee, and E. A. Bazaev, *J. Chem. Eng. Data* **46**:1610 (2001).
60. W. Wagner and A. Pruß, *J. Phys. Chem. Ref. Data* **31**:387 (2002).
61. A. R. Bazaev, *Heat Transfer* **1**:113 (1988).
62. M. E. Fisher and G. Orkoulas, *Phys. Rev. Lett.* **85**:696 (2000).
63. Y. C. Kim, M. E. Fisher, and G. Orkoulas, *Phys. Rev. E* **67**:061506 (2003).
64. M. A. Anisimov and J. Wang, *Phys. Rev. Lett.* **97**:025703-1 (2006).
65. R. Fischer and T. Reichel, *Mikrochemie* **31**:102 (1943).
66. A. Battelli, *Mem. Torino* **44**:57 (1893).
67. R. F. Mocharnyuk, *Zh. Obsh. Khim.* **30**:1098 (1960).
68. R. C. Wilhoit and B. J. Zwolinski, *J. Phys. Chem. Ref. Data* **2**:(1973), Supplement I.
69. D. J. Rosenthal and A. S. Teja, *Ind. Eng. Chem. Res.* **28**:1693 (1989).
70. T. Hu, Zh. Qin, G. Wang, X. Hou, and J. Wang, *J. Chem. Eng. Data* **49**:1809 (2004).
71. S. M. Loktev, *High Fat Alcohols* (Khimiya, Moscow, 1970).
72. Yu. V. Efremov, *Russ. J. Phys. Chem.* **40**:1240 (1966).
73. S. Young, *Sci. Proc. Roy. Dublin Soc.* **21**:374 (1910).
74. J. Griswold, J. D. Haney, and V. A. Klein, *Ind. Eng. Chem.* **35**:701 (1943).
75. A. Z. Golik, S. D. Ravikovich, and A. V. Orishchenko, *Ukr. Khim. Zh.* **21**:167 (1955).
76. V. F. Nozdrev, *Akust. Zh.* **2**:209 (1956).
77. W. Ramsay and S. Young, *Phyl. Trans. Roy. Soc. (London) A* **178**:313 (1887).
78. L. Crismer, *Bull. Soc. Chim. Belg.* **18**:18 (1904).
79. M. T. Rätzsch and G. Strauch, *Z. Phys. Chem. (Leipzig)* **249**:243 (1972).
80. W. L. Marshall and E. V. Jones, *Inorg. Nucl. Chem.* **36**:2319 (1974).
81. H. K. Ross, *Ind. Eng. Chem.* **46**:601 (1954).
82. K. A. Kobe and R. E. Lynn, *Chem. Rev.* **52**:117 (1953).